第 28 卷 第 5 期
2007 年 5 月

半 导 体 学 报
CHINESE JOURNAL OF SEMICONDUCTORS

Vol.28 No.5
May,2007

# A $Q$-Enhanced CMOS RF Filter for Multi-Band Wireless Communications

Gao Zhiqiang[1,†], Yu Mingyan[1], Ma Jianguo[2], and Ye Yizheng[1]

(1 *Microelectronics Center*, *Harbin Institute of Technology*, *Harbin* 150001, *China*)
(2 *Institute of Electronic Engineering*, *University of Electronic Science and Technology of China*, *Chengdu* 610054, *China*)

**Abstract**: An RF bandpass filter with a $Q$-enhancement active inductor is presented. The design technique for a tunable $Q$-enhancement CMOS active inductor operating in the wide RF-band is described. Moreover, issues related to noise and stability of the active inductor are explained. The filter was fabricated in 0.18$\mu$m CMOS technology, and the circuit occupied an active area of only 150$\mu$m $\times$ 200$\mu$m. Measurement results show that the filter centered at 2.44GHz with about 60MHz bandwidth (3dB) is tunable in center frequency from about 2.07 to 2.44GHz. The 1dB compression point is $-15$dBm while consuming 10.8mW of DC power, and a maximum quality factor of 103 is attained at the center frequency of 2.07GHz.

**Key words**: active inductor; RF bandpass filter; 1dB compression point; quality factor; CMOS process
**EEACC**: 1230B; 2570K
**CLC number**: TN75  **Document code**: A  **Article ID**: 0253-4177(2007)05-0670-06

## 1 Introduction

In recent years, motivated by the growing wireless communication business, much effort has been devoted to the implementation of highly integrated, low-cost RF components in CMOS technology. One of the factors limiting the integration of RF transceivers is the low quality of passive components in commercially available IC processes. Realization of on-chip RF bandpass filters required for narrow band-selection, low insert-loss, low intermodulation distortion, and noise figure, is undoubtedly one of the most challenging tasks in realizing low-cost CMOS front-end transceiver for wireless communications. In many contemporary receivers, this necessitates the use of on-chip passive spiral inductors to achieve good matching and power gain[1~8], because active inductors on-chip have great difficulty emulating spiral inductors. However, spiral inductors suffer from wiring and substrate losses, rendering a low quality factor. $Q$-enhancement active circuitry is usually employed to boost the quality factor at the cost of noise, linearity, additional processing steps, power dissipation, and reliability problems[3,5,6,9]. Although the problems have been addressed by using various passive methods such as patterned ground shields and geometry improvements[10], the $Q$ factor of integrated inductors is still generally limited to a value less than 20 in standard RF CMOS processes[11]. Furthermore, spiral inductors require large chip area, and their tunable modeling is not good.

The above difficulties can be overcome by using an active inductor, which offers wide-tuning ability and high quality factor under small chip area. Recent research on Si-integrated inductor design has an increasing interest in the design and implementation of CMOS inductorless RF bandpass filters[12~14].

In this paper, we describe the design of a tunable $Q$-enhancement integrated inductorless filter that provides high band-selection. The design of the proposed active inductor is also given, and it is followed by the noise analysis of the $Q$-enhanced active inductor. Additionally, the stability of the filter is addressed. Then the prototype design of the RF filter and measured results are presented.

† Corresponding author. Email: gao_zhiqiang@hit.edu.cn
Received 9 November 2006, revised manuscript received 17 January 2007

# 2 Circuit principle

## 2.1 Proposed active inductor and noise analysis

Inductors are often fabricated by combining a gyrator and capacitor. But designing high-$Q$ active inductors at GHz with opamps or standard transconductance-$C$ techniques is very difficult due to relatively significant power consumption and noise. Active inductors based on the principle of gyration, consisting of single or minimum-count transistors, can be operated at GHz easily because $f_T$ of a single transistor is as high as hundreds of GHz.

A class of active inductors that has been proposed by researchers[12~14] is shown in Fig. 1. A common feature of these active inductor topologies is that they all employ some kind of shunt feedback to emulate the inductive impedance. Comparing the active inductors shown in Fig. 1(a) and the improved versions in Figs. 1(b) and (c), we found that the active inductor in Fig. 1(a) has the least transistor-count, and its noise is lower than the active inductors in Figs. 1 (b) and (c). As can be seen from the circuit diagram, the minimum voltage for the active inductor itself is the least. Therefore, the circuit in Fig. 1 (a) is better than the circuits in Fig. 1 (b) or (c), and it has two transistors contributing noise directly to the input. In our design, the current-reused active inductor based on Fig. 1 (a) is chosen. A more detailed small-signal representation of Fig. 1 (a) is shown in Fig. 2, where $g_o$ is the drain-source conductance (i.e. $g_{o1}$ and $g_{o2}$ as shown in Fig. 2) and $g_{oc}$ represents the loading effect of the non-ideal biasing current source. The inductive impedance of $Z_{in}$, i.e. $Z_L$, can be expressed as

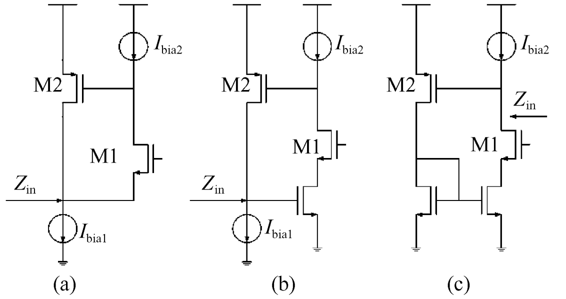


Fig. 1　CMOS active inductors

$$Z_L = \frac{g_{oc} + g_{o1} + s(C_{gs2} + C_{gd2} + C_{ds1})}{g_{m1} g_{m2} + [g_{m2} - g_{m1} + g_{oc} + s(C_{gs2} + C_{ds1})](g_{o2} + sC_{gd2})} \tag{1}$$

The small-signal analysis of the circuit in Fig. 2 shows that $Z_{in}$ is a parallel RLC resonant tank with the following values:

$$R_p = \frac{1}{g_{o2}} \parallel \frac{1}{g_{m1}} \approx \frac{1}{g_{m1}} \times C_p \approx C_{gs1} L_p \approx \frac{C_{gs2}}{g_{m1} g_{m2}} r_L = \frac{g_{oc} + g_{o1}}{g_{m1} g_{m2}} \tag{2}$$

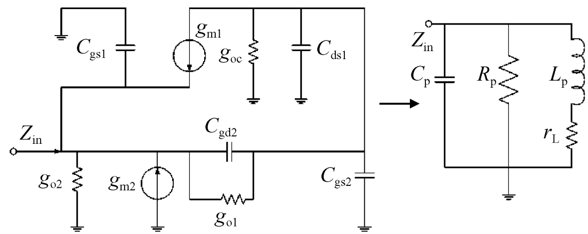


Fig. 2　Small-signal equivalent circuit

The self-resonant frequency $\omega_0$ and intrinsic quality-factor of the inductor are

$$\omega_0 \approx \sqrt{\frac{g_{m1} g_{m2}}{C_{gs1} C_{gs2}}} = \sqrt{\omega_{t1} \omega_{t2}} \tag{3}$$

$$Q_0 = \frac{R_p}{\omega_0 L_p} \approx \sqrt{\frac{g_{m2} c_{gs1}}{g_{m1} c_{gs2}}} \tag{4}$$

where $\omega_{t1}$ and $\omega_{t2}$ are the unity-gain frequencies of M1 and M2, respectively. Although an active inductor can provide the necessary reactance through the gyrator-$C$ principle, the relatively large noise and low dynamic range of the active inductor will limit its performance. Unlike the passive inductor, where the damping resistor $r_L$ is the main noise contributor, the noise in an active inductor originates from the thermal noise of the MOS transistor channel[9,14]. By referring the transistor noise sources to the terminals of the active inductor in Fig. 1(a), where $\overline{v_{n1}^2} = 4kT\varepsilon\Delta f / g_{m1}$, $\overline{i_{n2}^2} = 4kT\varepsilon g_{m2}\Delta f$, $kT$ is Boltzmann's constant times temperature in Kelvin, and $\varepsilon$ is chosen empirically to match the observed thermal noise behavior of a given fabrication process. The total mean-squared noise voltage generated by the intrinsic active inductor at its input node in the whole frequency can be expressed as

$$\overline{V_{n,L}^2} = \varepsilon kT\left(\frac{1}{C_{gs1}} + \frac{1}{C_{gs2}}\right)\frac{g_{m2}}{g_{m1}} \tag{5}$$

We find that the high ratio of $g_{m2}/g_{m1}$ will degrade the noise performance. Simultaneously, as can be seen by Eqs. (1)～(4), the inductance contribution $Z_L$ has one zero and two poles. The zero is located at $\omega_Z = (g_{oc} + g_{o1})/(C_{gs2} + C_{gd2} + C_{ds1})$ and $\omega_p \approx \omega_t$. Therefore, the inductive circuit can obtain very high frequency and wide operating bandwidth from $\omega_Z$ to $\omega_P$ through increasing $g_m/C$ (the ratio of the transconductance and the gate-source capacitor of M1 or M2), but the quality factor of the circuit will be degraded according to Eq. (4). However, a high quality factor is required for RF filters. To further enhance the $Q$ and avoid issues related to the noise and instability when we introduce negative impedance techniques[4,12～14], the trade-offs between noise, $Q$-enhancement and stability should be taken into account.

### 2.2 Q-enhanced technique and stability analysis

Since the basic concept in the $Q$-enhanced LC filter is to use a lossy LC tank, it is necessary to implement a loss compensation to boost the filter quality factor incorporating negative-conductance. Negative conductance $g_{mn}$ (M7, M8, M9, M10 as shown in Fig. 3) realizes the required negative resistance to compensate for the loss in the tank. The effective quality factor[4] of the filter at the resonant frequency can be shown to be

$$Q_{en} = \frac{Q_c}{1 - g_{mF} R_p} \tag{6}$$

where $Q_c$ is the base quality factor of the LC tank, which is dominated by the equivalent inductor. Theoretically, it can be set as high as desired with appropriate $g_{mn}$. Indeed, the filter core can be tuned to oscillate if negative transconductance is sufficiently large, i.e., greater than $1/R_P$.

Additionally, the main problem is that the use of shunt-shunt feedback by M2 to compensate the loss resistance of the active inductor can result in potential instability, depending on the filter terminating impedances. In order to make sure that the circuit is stable, the magnitude of the input reflection coefficient must be less than unity, i.e. $|S_{11}| < 1$. According to Eq. (1) using closed-loop analysis, the circuit will be stable provided that

$$g_{m1} < \frac{(C_{gs2} + C_{ds1}) g_{o2}}{C_{gd2}} + g_{m2} + g_{oc} \tag{7}$$

Due to the stability problem, we should determine the reasonable transconductance $g_{m1}$ and $g_{m2}$ in order that the trade-offs between noise, $Q$-enhancement, and stability will satisfy the requirements of communication systems.

## 3 Design of the RF filter and measured results

### 3.1 Circuit design

The complete prototype circuit of the proposed second-order RF bandpass filter based on the active inductor is shown in Fig. 3. This circuit consists of three different stages, including two differential high $Q$-enhancement active inductors, negative impedance, and buffers. Common-drain transistors M11, M13 and M12, M14 are employed for the output buffer stages. This common drain configuration can accomplish loading effect minimization and 50Ω output impedance matching. The output buffer stages will cause about 15dB loss when driving a 50Ω load.

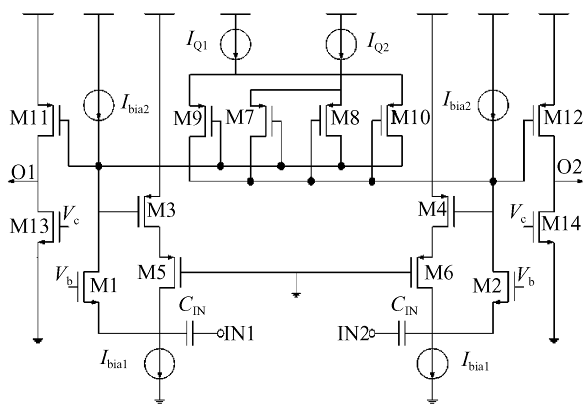


Fig. 3 A $Q$-enhancement RF bandpass filter

M1, M3, M5 and M2, M4, M6 construct an LC-resonant circuit which is made up of the active inductors. M7, M8 and M9, M10 consist of a cross-coupled pair and are employed to produce not only a negative resistance for reducing the inductor loss, but also increased linearity of the filter when the signal is large. Note that the DC bias current $I_{Q1}$ and $I_{Q2}$ can be used to control the $Q$ of the inductor and the transconductance of the cross-coupled pairs[14]. $V_b$, $V_c$ are bias voltages which are used for the DC operating state of the filter. The DC bias currents $I_{bia1}$ and/or $I_{bia2}$ can be adjusted to tune the center frequency of the circuit and also enhance the $Q$ of the inductance shown in Fig. 3. As a matter of fact, the filter in Fig. 3 consists of RLC resonators with two input ports. It uses a positive feedback with M7, M8 and M9, M10 to compensate the internal loss of the active inductor, and the gain of the circuit is increased at the same time.

### 3.2 Measured results

The circuit is fabricated in a 0.18μm UMC-HJTC CMOS process through the educational service. Figure 4 shows a microphotograph of the fabricated circuit. To ensure the fully differential operation, a symmetrical layout is used for the design. The total chip area is 0.7mm × 0.75mm including the pads, where the active area occupies only 0.15mm × 0.2mm. RF signal path measurements were made with an on-wafer probe station, and G-S-G probes. The two-port *S*-parameter measurements were made with an Agilent E8363B vector network analyzer. Noise measurements were made with a spectrum analyzer equipped with power measurement software and a noise source. The 1dB compression point measurements were made with a spectrum analyzer and a power meter.

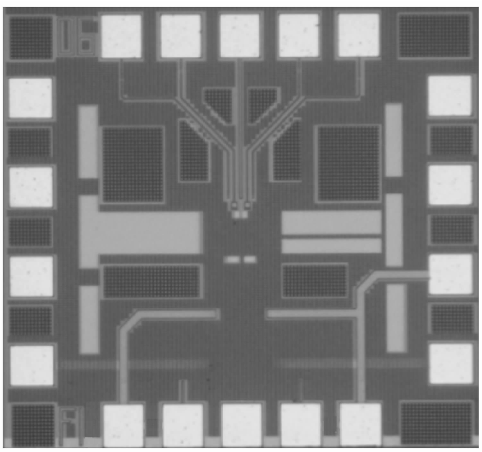

Fig.4　Microphotograph of the fabricated RF filter

The measured RF bandpass filter forward transmission response, $S_{21}$, is shown in Fig. 5 and Fig. 6, respectively. Figure 5 shows that the passband center frequency is 2.07GHz, and the 3dB bandwidth is about 20MHz. The maximum gain in the passband is about 25.25dB. It should be noted that the input return loss, $S_{11}$ is only − 8.674dB in Fig. 5 with a noise figure of about 22dB and an output return loss of about − 4dB. The *Q* of the RF filter is very high, but at the expense of potential instability and a large noise figure. Figure 6 shows that the passband center frequency is about 2.44GHz and the 3dB bandwidth is about 60MHz. The maximum gain in the passband is about 5.991dB, and the input/output return loss is about − 18.7dB/ − 14.3dB. The tenability of the RF filter in Fig. 6 shows the AC tuning response of the filter in the tuning center frequency from about 2.07 to 2.44GHz when the DC voltage sources of the controlled bias current $I_{\text{bia1}}$ and/or $I_{\text{bia2}}$ is adjusted from 0.5 to 1.5V and the voltage value of the controlled $I_{Q1}$ and $I_{Q2}$ varies from 0 to 0.5V or vice versa. Figure 7 shows that the input impedance of the RF filter has the behavior of an inductor at the tuning frequency range from 2.07 to 2.4GHz because the input return loss $S_{11}$ is located at the part of inductance from the Smith Chart. Good input match has not been achieved over the filter passband because the probe pads and connecting traces to the filter do not present true 50Ω termination impedance, resulting in return loss at the input terminals.

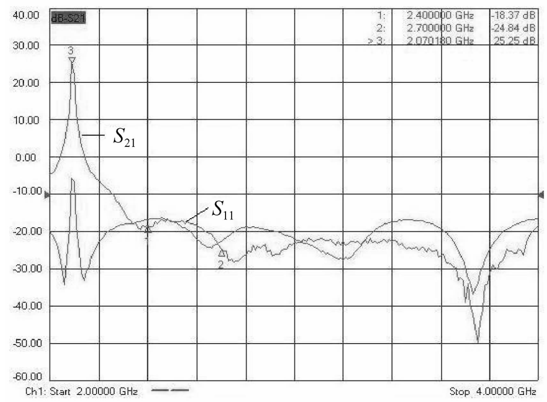


Fig.5　Measured bandpass filter insertion loss, $S_{21}$ at 2.07GHz

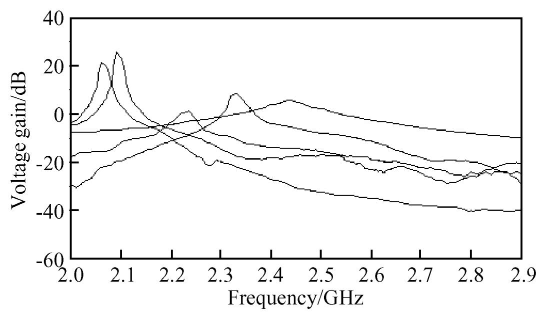


Fig.6　Measured RF filter response versus frequency tuning

A measurement of the 1dB compression point of the circuit can be obtained by sweeping the in-

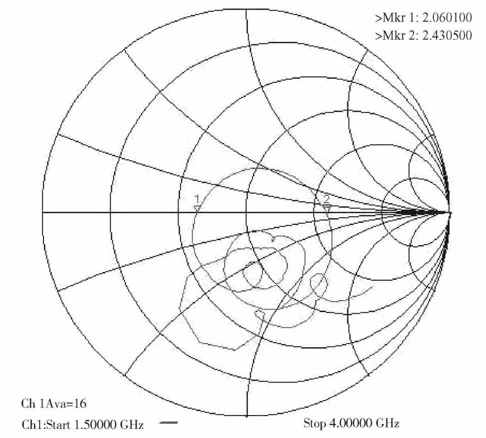


Fig. 7 Measured bandpass filter input return loss, $S_{11}$

put power to the tank and measuring the output power. As the input power is increased, the input impedance presented by the $Q$-enhanced active inductor tanks begins to drop due to nonlinear effects, which can be observed when the output power no longer depends on the input power in a linear fashion as shown in Fig. 8. The measured

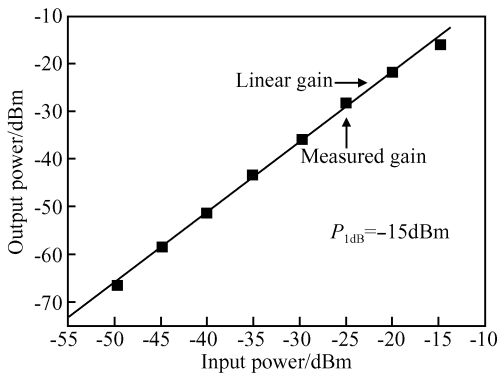


Fig. 8 Measured bandpass filter 1dB compression at 2.44GHz

bandpass filter $P_{1\mathrm{dB}}$ input power compression point is $-15$dBm at the center 2.44GHz passband. The noise figure of 18dB was also measured by disconnecting the input signal.

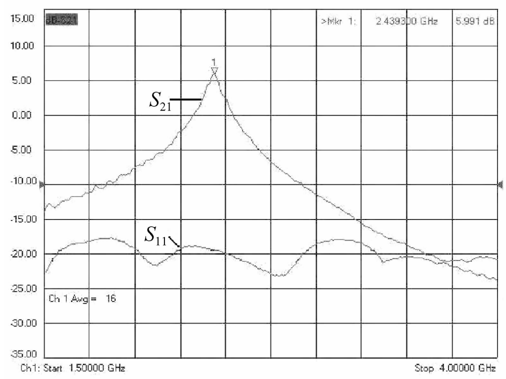


Fig. 9 Measured bandpass filter insertion loss, $S_{21}$ at 2.44GHz

Table 1 summarizes the performance of the fabricated filters in CMOS and other processes in the literature. A figure of merit[5] (FOM) which allows comparison between other RF filters in silicon is given as

$$\mathrm{FOM} = \frac{NP_{1\mathrm{dBW}} f_{\mathrm{center}} Q_{\mathrm{filter}}}{P_{\mathrm{DC}}\mathrm{NF}} \tag{8}$$

where $N$ is the number of poles, $P_{1\mathrm{dBW}}$ is the in-band 1dB compression point in Watts, $f_{\mathrm{center}}$ is the center frequency, $Q_{\mathrm{filter}}$ is the ratio of the center frequency and the 3dB bandwidth, NF is the noise factor, and $P_{\mathrm{DC}}$ is the DC power dissipation.

Table 1 shows that the filter presented in this work achieves a good FOM with a high quality factor, high gain in the passband, wide tuning range, and the smallest chip area.

Table 1 Comparison of the RF bandpass filters performance

| Reference | Process | $f_0$/GHz | Bandwidth /MHz | $V_{\mathrm{dd}}$/V | Die area /mm$^2$ | Tuning range /MHz | Midband gain /dB | FOM/dB |
|---|---|---|---|---|---|---|---|---|
| Ref. [5] | 0.18$\mu$m CMOS | 2.03 | 130 | 1.8 | 0.81 | 60.9 | 0 | 77 |
| Ref. [6] | 0.18$\mu$m CMOS | 2.36 | 60 | 1.8 | 2.25 | 0 | −1.8 | 78 |
| Ref. [7] | 0.5$\mu$m Si-SOI | 2.5 | 70 | 3 | 2.5 | 250 | 14 | 82 |
| Ref. [8] | 0.25$\mu$m CMOS | 2.14 | 60 | 2.5 | 3.5 | 0 | 0 | 72 |
| This work | 0.18$\mu$m CMOS | 2.44 | 60 | 1.8 | 0.53 | 370 | 6 | 81 |

## 4 Conclusion

The design and implementation of a tunable RF bandpass filter in a 0.18μm CMOS process have been introduced and verified. It has been demonstrated that it can achieve a very high quality factor with 6mA current and 1.8V supply and has a large tuning range from 2.07 to 2.44GHz. Although the noise and linearity of the proposed active inductors are inferior to passive ones, the small chip area and high tenability make them applicable in multi-band on-chip wireless systems in future.

**Acknowledgment** The author would like to thank Professor Liu Xinyu, Yang Chengyue from the Institute of Microelectronics, Chinese Academy of Sciences and Professor Wang Zhigong, Li Wei from Southeast University for valuable guidance and help in measurement of the chip.

### References


[1] Dulger F, Sinencio E, Silva-Martinez J. A 1.3V 5mW fully integrated tunable bandpass filter at 2.1GHz in 0.35μm CMOS. IEEE J Solid-State Circuits, 2003, 38: 918

[2] Georgescu B, Pekau H, Haslett J, et al. Tunable coupled inductor *Q*-enhancement for parallel resonant LC tanks. IEEE Trans Circuits Syst II, 2003, 50: 705

[3] Kuhn W B, Nobbe D, Kelly D, et al. Dynamic range performance of on-chip RF bandpass filters. IEEE Trans Circuits Syst II, 2003, 50: 685

[4] Kuhn W, Stephenson F, Elshabini-Riad A. A 200MHz CMOS *Q* enhanced LC bandpass filter. IEEE J Solid-State Circuits, 1996, 31: 1112

[5] Georgescu B, Finvers I G, Ghannouchi F. 2GHz *Q*-enhanced active filter with low passband distortion and high dynamic range. IEEE J Solid-State Circuits, 2006, 41: 2029

[6] Kulyk J, Haslett J. A monolithic CMOS 2368±30MHz transformer based *Q*-enhanced series-C coupled resonator bandpass filter. IEEE J Solid-State Circuits, 2006, 41: 362

[7] He X, Kuhn W B. A 2.5GHz low-power, high dynamic range, self-tuned *Q*-enhanced LC filter in SOI. IEEE J Solid-State Circuits, 2005, 40: 1618

[8] Soorapanth T, Wong S S. A 0-dB IL, 2140±30MHz bandpass filter utilizing *Q*-enhanced spiral inductors in standard CMOS. IEEE J Solid-State Circuits, 2002, 37: 579

[9] Abidi A A. Noise in active resonators and the available dynamic range. IEEE Trans Circuits Syst I, 1992, 39: 296

[10] Yue C P, Wong S S. On-chip spiral inductors with patterned ground shields for Si-based RFICs. IEEE J Solid-State Circuits, 1998, 33: 743

[11] Cao Y, Groves R A, Huang X, et al. Frequency-independent equivalent-circuit model for on-chip spiral inductors. J Solid-State Circuits, 2003, 38: 419

[12] Gao Z H, Ma J G, Yu M Y, et al. A CMOS RF bandpass filter based on the active inductor. Proc 2005 6th Int Conf ASIC, Shanghai, 2005: 604

[13] Wu Y, Ismail M, Olsson H. A novel CMOS fully differential inductorless RF bandpass filter. Proc IEEE Int Symp Circuits Syst, Switzerland, 2000: 149

[14] Wu Y, Ding X, Ismail M, et al. RF bandpass filter design based on CMOS active inductors. IEEE Trans Circuits Syst II, 2003, 50: 942


# 一种适用于多波段无线通信的品质因数增强型的 CMOS 射频滤波器


高志强[1,†]　喻明艳[1]　马建国[2]　叶以正[1]

(1 哈尔滨工业大学微电子中心，哈尔滨　150001)

(2 电子科技大学电子工程学院，成都　610054)


**摘要**：提出了一种使用品质因数增强型的有源电感的射频带通滤波器，描述了在宽射频频段上可调谐的品质因数增强型的有源电感设计技术，而且解释了与有源电感噪声和稳定性相关的问题. 该滤波器采用 0.18μm CMOS 工艺制造，它所占用芯片的有效面积仅为 150μm×200μm. 测试结果表明：该射频滤波器中心频率为 2.44GHz 时，3dB 带宽为 60MHz，中心频率可在 2.07～2.44GHz 范围内调谐，1dB 压缩点为 −15dBm，而静态功耗为 10.8mW；在中心频率为 2.07GHz 时，滤波器的品质因数可达到 103.

**关键词**：有源电感；射频带通滤波器；1dB 压缩点；品质因数；CMOS 工艺

**EEACC**：1230B；2570K

**中图分类号**：TN75　**文献标识码**：A　**文章编号**：0253-4177(2007)05-0670-06

† 通信作者. Email: gao_zhiqiang@hit.edu.cn

2006-11-09 收到，2007-01-17 定稿